# Dynamic response of detached recombining plasmas to plasma heat pulse in a divertor simulator

N. Ohno,[a] M. Tanaka, N. Ezumi, D. Nishijima, and S. Takamura
*Department of Energy Engineering and Science, Graduate School of Engineering, Nagoya University, Nagoya 464-8603, Japan*

S. I. Krasheninnikov and A. Yu. Pigarov
*Plasma Science and Fusion Center, Massachusetts Institute of Technology, Cambridge, Massachusetts 02139*

J. Park[b]
*Princeton Plasma Physics Laboratory, Princeton University, Princeton, New Jersey 08543*

(Received 14 May 1998; accepted 26 February 1999)

The experiments on the plasma heat pulse to the detached recombining helium plasma associated with the volumetric radiative and three-body recombination (EIR) have been performed in a linear divertor plasma simulator. Detailed observations of the time evolution of plasma parameters and helium Balmer series spectra show that the dynamic response of the detached recombining plasma to the heat pulse depends strongly on the heat transport through energetic electrons generated by the heat pulse. For the detached recombining plasma with a relatively low neutral pressure, it was found that the EIR is not sufficient to suppress an increase of ion flux to the target plate during the pulse. Several key characteristic time scales involved in this system are also analyzed. © *1999 American Institute of Physics.* [S1070-664X(99)01606-7]

## I. INTRODUCTION

In recent years, the investigation of plasma detachment has received considerable attention, particularly in the edge plasmas of magnetic confinement fusion devices. Plasma detachment is thought to be one of the most effective methods to reduce the plasma heat flux to plasma-facing components.[1–5] Recent studies on detached plasmas in fusion-related divertor plasma experiments indicate that volumetric plasma recombination in detailed plasmas plays an essential role in the strong reduction of ion particle flux along the magnetic field, resulting in a decrease in the heat flux to plasma-facing components.[6–14] In tokamaks with a divertor configuration and in linear divertor plasma simulators, continuum and series of visible line emissions from highly excited levels due to the radiative and three-body recombination (referred to as EIR hereafter) were clearly observed in detached plasmas. On the other hand, a new recombination process associated with excited hydrogen molecules, the so-called molecular activated recombination (MAR), was theoretically predicted in divertor plasma conditions.[15–17] Recent experimental results gave the evidence of the MAR.[12,14]

In the next generation fusion devices, which are intended to have a steady state operation, we should do well both in the reduction of plasma heat flux with the plasma detachment and good confinement, such as the high-confinement mode (*H*-mode). Coexistence of the detached recombining plasma and good confinement in a tokamak was demonstrated in the Axisymmetric Divertor Experiment (ASDEX)-Upgrade tokamak as the completely detached *H*-mode (CDH) with a precise feedback control of impurity injection,[18] and well reproduced in the DIII-D tokamak.[19] In the design activity of the International Thermonuclear Experimental Reactor (ITER),[20] *H*-mode with edge localized mode (ELM), which brings an intermittent plasma heat pulse in the divertor plasma region, is one of the most important operation candidates as a good stationary confinement mode. Therefore, it is one of the most urgent issues to understand the dynamics of the detached recombining plasma to the intermittent plasma heat pulse associated with an ELM. In particular, we should make it clear that the volumetric plasma recombination, especially EIR, may work well for the intermittent plasma heat pulse, so that the ion particle flux and heat load to the divertor plate may be reduced enough. However, there is no clear investigation on the behavior of detached recombining plasma associated with the plasma heat pulse so far.

In this paper, we report on the dynamic response of the detached recombining plasma associated with EIR in the linear divertor plasma simulator, Nagoya University Divertor Simulator (NAGDIS-II).[11] In the present case, we examine pure helium plasmas, in which there are no MAR processes and only EIR is responsible for the plasma detachment. The time evolution of plasma parameters and the helium Balmer series spectra are found to depend strongly on the neutral pressure in the divertor plasma test region. For the detached recombining plasma at a relatively low neutral pressure, it is found that the EIR does not work well enough to suppress an increase of ion flux to the target plate during the heat pulse. Detailed analysis of characteristic time scales involved in the system shows that the time evolution of the detached recom-

[a]Electronic mail: ohno@nuee.nagoya-u.ac.jp
[b]Present address: Los Alamos National Laboratory, Los Alamos, New Mexico 87545.

 

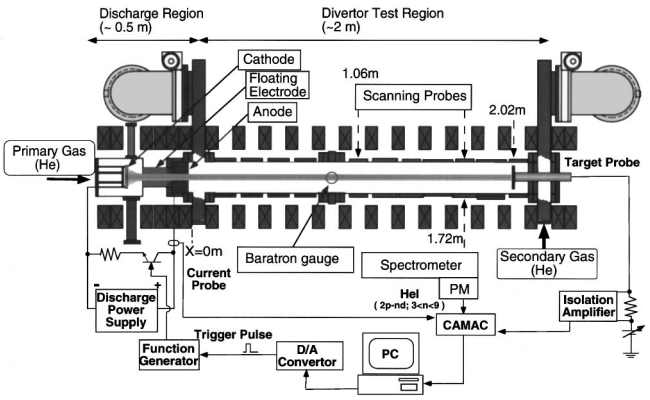


FIG. 1. Schematic of the experimental apparatus, NAGDIS-II.

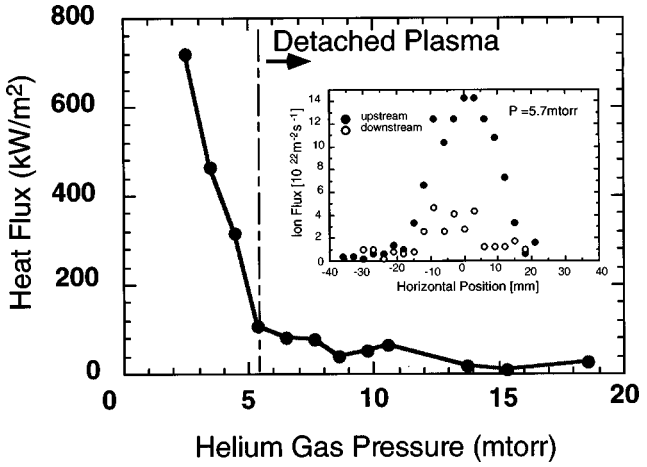


FIG. 2. Averaged heat load to the target plate as a function of the neutral gas pressure $P$ in the divertor test region. The horizontal profiles of ion flux measured at upstream ($X$=1.06 m) and downstream ($X$=1.72 m) are illustrated in the inset.

bining plasma is mainly determined by the heat pulse transport through the electron channel, including the energetic electron contribution. Relatively small concentrations of the energetic electrons originally coming from the plasma source region are shown to play an important role in the detached plasma dynamics.

## II. EXPERIMENTAL SETUP

The experiments were performed in the linear divertor plasma simulator, NAGDIS-II. The schematic of the experimental setup is shown in Fig. 1. The base pressure of the vacuum chamber equipped with two 2000 ℓ/s turbomolecular pumps is less than $10^{-7}$ Torr. The magnetic field strength is 0.25 T. Helium is introduced as a primary gas at a pressure of ~1.0 Torr into the discharge region to generate helium plasmas by the improved test plasma by direct-current discharge (TP-D) type discharge with a focusing magnetic field.[21] High density plasmas produced in the discharge region are introduced into the divertor test region through the apertures of the electrically floated intermediate electrode and the anode, whose diameters are 0.02 m and 0.024 m, respectively. The plasma density can be controlled by changing a discharge current $I_p$. The plasma column is terminated by the target plate, with water cooling installed at the end of the vacuum chamber. The neutral pressure $P$, measured with a baratron pressure gauge, in the divertor test region is kept less than 1 mTorr, even when the discharge is on, and can be controlled from 1.0 mTorr to 20.0 mTorr by feeding a secondary gas near the target plate. It should be noted that the change of $P$ in the divertor test region has no effect on the plasma production in the plasma source region due to three orders of magnitude pressure difference between the plasma source and the divertor test region.

Plasma heat pulse is produced by modulating the discharge current $I_p$, which is realized by switching the giant transistor connected parallel to the discharge circuit as shown in Fig. 1. The $I_p$ is monitored by a current probe.

The spectra of visible light emissions from helium atoms are detected at the axial position of $X$=1.72 m downstream from the discharge anode electrode. Fast scanning probes are installed at the axial positions of $X$=1.06 m and $X$=1.72 m to measure plasma parameters. Ion fluxes to the target plate ($X$=2.02 m) are measured with the flush mounted probe on the target plate, and time-averaged heat load to the target plate is estimated by measuring the temperature rise of the cooling water, the so-called calorimetry method.

## III. EXPERIMENTAL RESULTS

### A. Characteristics of stationary detached recombining plasma

First we investigate the basic characteristics of the detached plasmas in a steady state, because it gives us the basis for understanding of the dynamic behavior of recombining plasma, which will be described in the next section. Plasma detachment is achieved by feeding the secondary gas near target plate. Figure 2 shows the dependence of the heat load to the target plate on the helium gas pressure $P$ at a discharge current $I_p$of 50 A. With an increase in $P$, the heat load is found to drop rapidly, and at $P$~5.0 mTorr, to be an order of magnitude smaller than that of the initial value. At this pressure, we can observe that the plasma starts to detach from the target plate. Very bright visible light emissions in front of the target plate were observed with the naked eye. A further increase in $P$ leads to making the bright emission region (detached region) go away from the target plate, then a clear dark region appears between the target plate and the region with the bright visible emissions. The spatial extent of the bright zone is about 30 cm, and the viewing chord of the spectrometer sees the bright zone for the pressure range from 5 mTorr to 12 mTorr. The horizontal profiles of ion flux measurement at upstream ($X$=1.06 m) and downstream ($X$=1.72 m) are also illustrated in the inset of Fig. 2 at a neutral pressure $P$ of 5.7 mTorr. Figure 3 shows the spectrum of visible light emission from 310 nm through 370 nm observed in the detached region at $P$ of 5.4 mTorr and a discharge current $I_p$ of 50 A, compared to the spectrum without the secondary helium gas puff at $P$~1.0 mTorr. At $P$~1.0 mTorr, the plasma column had an electron temperature $T_e$ of 5 eV and a plasma density $n_e$ of $0.8\times10^{19}$ $m^{-3}$. Here, the emission lines from the low excited states dominate the spectrum, indicating that excited levels are populated by electron

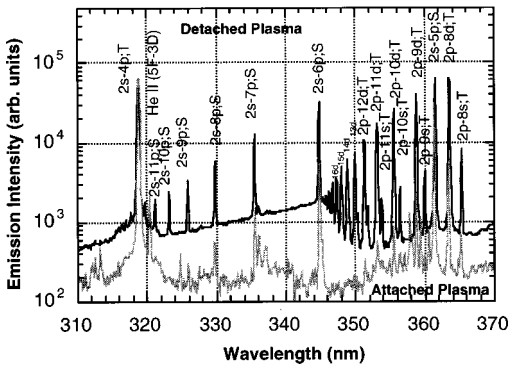


FIG. 3. Visible light emission spectra from helium plasma with a helium gas puff at $P\sim5.4$ mTorr and without a helium gas puff at $P\sim1.0$ mTorr.

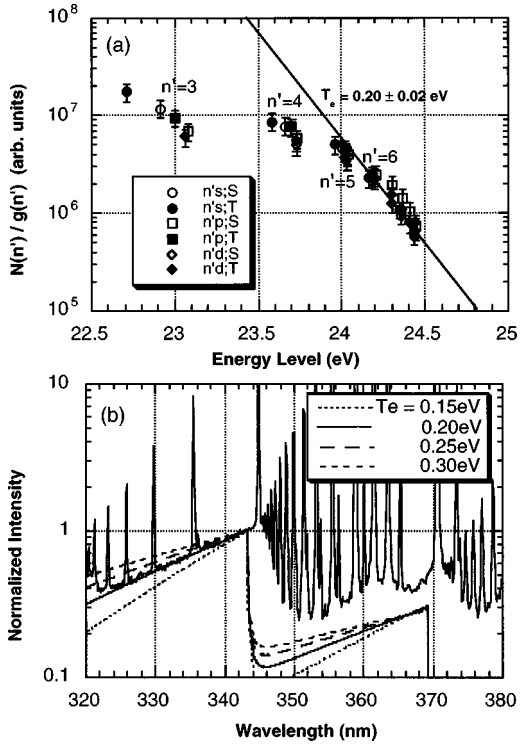


FIG. 4. (a) Dependence of relative population densities of helium Balmer series per unit statistical weight as a function of the energy level at $P\sim5.4$ mTorr in steady state. (b) Comparison between the observed continuum spectrum and calculated ones with the CRAMD code at several electron temperatures.

impact excitation from the ground state. At $P\sim5.4$ mTorr, the emission spectrum from this detached region of the plasma shows a very prominent continuum radiation starting from 344 nm, connected to the He I $(2p-n'd;\ T)$ triplet series limit. We can distinguish the line emission up to $n'\sim21$. This experimental result indicates that the EIR occurs in the detached region and contributes to the reduction of ion flux and heat load to the target plate.

In general, in order to realize EIR in plasma, we should have high-density plasmas with a low electron temperature below 1 eV. In such a detached helium plasma regime, our recent experimental studies have shown that the electron-ion energy exchange process followed by the ion-neutral charge exchange is a key mechanism responsible for the electron temperature drop along the magnetic field to be $T_e$ below 1 eV.[22,23]

To determine the electron temperature, line emission spectrum measured between 250 and 800 nm was analyzed to calculate the population densities of excited levels of helium atoms. Balmer-type lines (transition from the upper levels to $n'\sim2$ level) of helium atoms were used to obtain the population densities of excited levels up to $n'\sim10$ including the angular momentum sublevels of *S*, *P*, and *D* for both singlet and triplet spin states. It is noted that the high neutral pressure in the divertor plasma test region makes the resonance line opaque and forbids a direct absolute measurement of the $n'\sim2$ level population. Figure 4(a) shows the measured population density per unit statistical weight as a function of the energy level. The population distribution among the highly excited states $(n'>5)$ follows the Saha–Boltzmann distribution very closely. This implies that those states are in local thermal equilibrium (LTE) with the free electrons in the plasma, so that the electron temperature may be obtained by the Boltzmann equation[24,25]

$$\frac{1}{kT_e}=\frac{\Delta\ln(N(n')/g(n'))}{\Delta E(n')}. \tag{1}$$

Thus, the electron temperature of $0.20\pm0.02$ eV was estimated in the detached region of the plasma column. In addition, Fig. 4(a) shows the deviation from the local thermodynamic equilibrium (LTE) condition occurs at the principal quantum number between $n'\sim5$ and $n'\sim6$.

The second method to determine the electron temperature is to compare the observed continuum spectrum with the theoretically calculated one. Figure 4(b) shows the comparison between the experimentally observed strong continuum spectrum, connected to the He I $(2p\text{-}n'd;\ T)$ triplet series limit, and the ones calculated with the Collisional Radiative Atomic Molecular Data model (CRAMD code) (Ref. 17) as a function of the electron temperature $T_e$. The intensities are normalized by the intensity at the wavelength of 343.3 nm. The numerical result at $T_e\sim0.2$ eV is found to match well, which is in good agreement with the electron temperature obtained from the analysis on the population density of the excited levels mentioned before.[13]

It should be also pointed out that the $T_e$ measured with conventional Langmuir probes shows a much higher value than that obtained with the above optical method because the current–voltage probe characteristics in the detached recombining plasma show a strong anomaly due to the sharp gradient of the plasma parameters along the magnetic field line.[26] It is necessary to carefully interpret the current–voltage characteristics to determine $T_e$ in the detached recombining plasmas.[27] In this paper, $T_e$ in the detached recombining plasma was always obtained with the optical measurements, while $T_e$ in the attached plasma was measured with the Langmuir probe. Plasma density in the detached plasma was estimated from the ion saturation current measured by the Langmuir probe and $T_e$ obtained with the optical method.

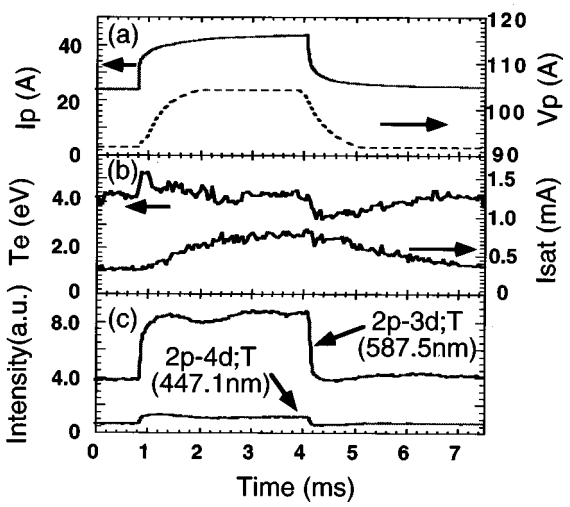


FIG. 5. Time evolution in an attached plasma ($P \sim 1.67$ mTorr) of (a) the discharge current $I_p$ and discharge voltage $V_p$; (b) the electron temperature $T_e$ measured with the Langmuir probe and the ion saturation current to the target plate $I_{sat}$; (c) the line emission intensities from the principal quantum number $n' = 3$ and 4.

### B. Time evolution of plasma parameters and line emission intensities in detached recombining plasmas

Plasma heat pulse was generated in the plasma source region by modulating the discharge current $I_p$, and was introduced into the attached and detached recombining plasmas in the divertor plasma test region. Figure 5 shows the time evolution of the discharge current $I_p$, the discharge voltage $V_p$, the ion particle flux $I_{sat}$ to the target plate, $T_e$ measured with the Langmuir probe, and the line emission intensities from excited states at the neutral helium pressure $P$ of 1.67 mTorr, when the plasma was attached to the target plate. The $I_p$ was changed from 24 A to 40 A with a duration time of about 3 ms by switching the giant transistor. At the same time, the discharge voltage $V_p$ was also changed automatically from 93 V to 105 V to sustain the change of $I_p$. Then, the total input power $W_p$ (defined by $I_p \times V_p$) during the heat pulse becomes 1.9 times as large as that without the heat pulse.

When the heat pulse enters ($I_p$ increases) at $t \sim 0.8$ ms, $T_e$ rapidly increases from 4 eV to 5 eV. After the $T_e$ peaks, $T_e$ is gradually decreasing during the heat pulse. Corresponding to the change in $T_e$, the line emission intensities from low quantum numbers $n' \sim 3$ and 4 show a steep increase at the beginning of the heat pulse. One of the reasons for this increase in the line emissions is thought to be that the rate coefficient of the electron impact excitation from the ground state $\langle \sigma v \rangle_{bulk}$ depends strongly on $T_e$ below 10 eV. During the heat pulse, the line emission intensities from low quantum numbers $n' \sim 3$ and 4 is almost constant, while $T_e$ is changed from 5 eV to 4 eV and the ion particle flux, which is roughly corresponding to the change of electron density $n_e$, increases to be twice as large as that at the beginning of the heat pulse. The rate coefficient of the electron impact excitation may decrease about one-fifth for the change in $T_e$ from 5 eV to 4 eV. Therefore, we cannot explain the constant line emission intensity by taking account of the time evolution of the bulk electron temperature and electron density because the line emission intensity is given by $\sim n_n n_e \langle \sigma v \rangle_{bulk}$, where $n_n$ is the neutral density. In order to quantitatively explain the change of the line emission intensities, we should also consider the contribution of energetic electrons (fast electrons) produced with the heat pulse in the plasma source region. This contribution will be discussed later. Anyway, at the beginning of the heat pulse, the input power is found to be mainly used to increase the kinetic energy of electrons. The line emission intensities from highly excited states above $n' \sim 5$ was quite small comparing to those from $n' \sim 3$ and 4.

On the other hand, $I_{sat}$ is gradually increasing during the heat pulse and decreasing after the heat pulse. In order to interpret the time evolution of $I_{sat}$, it is necessary to consider the effects of the convection of the plasma along the magnetic field, as well as the electron impact ionization. In the case of Fig. 5, $I_p$ and $I_{sat}$ start to increase at the same time. It takes more than 10 ms to transport the plasma from the plasma source region to the target plate, as is discussed in the next section. Therefore, we cannot explain the undelayed start-up of $I_{sat}$ by taking account of the plasma convection alone. The prompt start-up comes from the energetic electrons, which gain their energy due to the heat pulse, and may rapidly distribute over the divertor plasma test region to ionize the neutral particles all over the entire plasma volume. During the heat pulse, $I_{sat}$ is thought to be gradually increasing due to both effects of the ionization and the convection. When the heat pulse is terminated, $I_{sat}$ does not drop so rapidly in comparison with the change of $T_e$ because the plasma generated during the heat pulse in the upstream region flows into the target plate through the convection. On the other hand, $T_e$ rapidly goes down after the additional input power is terminated. Moreover, $T_e$ becomes below the initial value before the heat pulse. One of the reasons may be that the total input power to the electrons returns to the initial value, however the electron density remains at a higher value just after the heat pulse, resulting in lower input power per electron. The other reason may be that the electron cooling along the magnetic field lines due to the electron-ion thermalization process,[19] which is the dominant electron cooling channel below $T_e \sim 5$ eV in pure helium plasmas, is enhanced because the electron-ion thermalization time is proportional to $n_e^{-1}$. The characteristic time of the processes involved will be discussed in the next section in more detail.

In the case of a fairly detached plasma at $P \sim 6.25$ mTorr, the time evolution of line emission intensities is found to be dramatically changed as shown in Fig. 6, compared to those in Fig. 5. $T_e$ of the bulk plasma is about 0.3 eV before the heat pulse is on. At the beginning of the heat pulse, the line emission intensities from highly excited states above $n' \sim 5$ are found to drop in time, which means that the EIR becomes weak due to an increase in $T_e$ from 0.3 eV to 0.4 eV. On the other hand, the line emission intensities from low excited states $n' \sim 3$and 4 are increased, which cannot be explained by the change of the bulk electron temperature $T_e$ from 0.3 eV to 0.4 eV, because the rate coefficient of the electron impact excitation from the ground state is quite

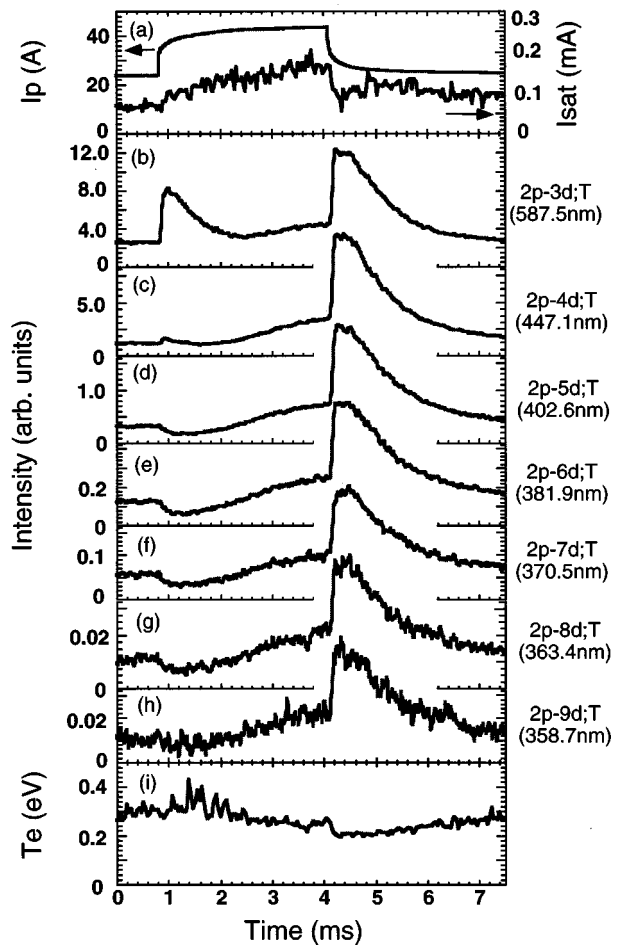


FIG. 6. Time evolution in a fairly detached plasma ($P \sim 6.25$ mTorr) of (a) the discharge current $I_p$ and the ion saturation current to the target plate $I_{sat}$; (b)–(h) the line emission intensities from principal quantum number $n'$ from 3 through 9; (i) the electron temperature $T_e$ measured with the optical method.

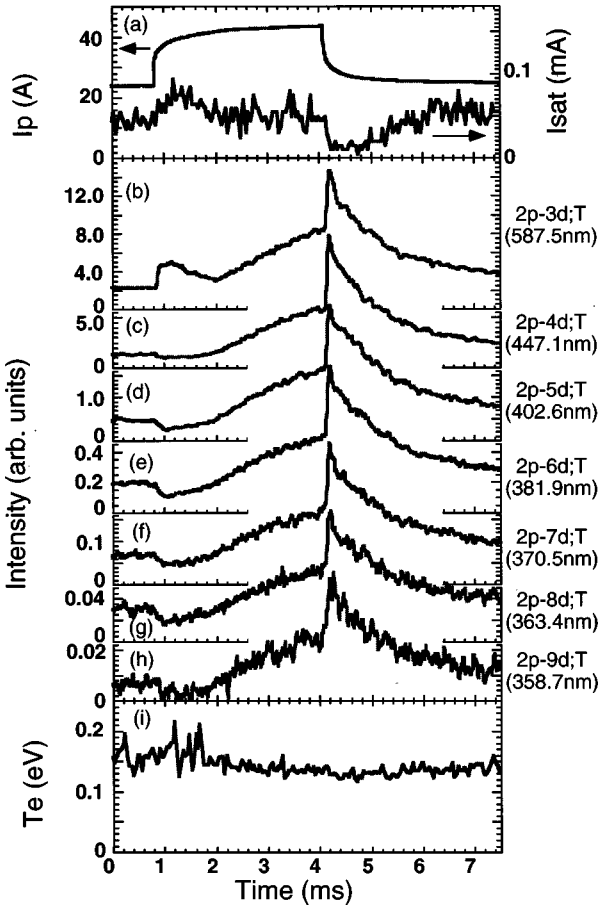


FIG. 7. Time evolution in a deeply detached plasma ($P \sim 9.46$ mTorr) of (a) the discharge current $I_p$ and the ion saturation current to the target plate $I_{sat}$; (b)–(h) the line emission intensities from principal quantum number $n'$ from 3 through 9; (i) the electron temperature $T_e$ measured with the optical method.

small in this temperature range in comparison with that of EIR, and the peak of the line emission intensities from low excited states $n' \sim 3$ and 4 does not coincide with that of the bulk electron temperature. This result also indicates that we should consider energetic electron components (fast electrons), which can excite neutrals in the detached plasma at the beginning of the heat pulse. In this case, the population density in low excited state $(n' \sim 3)$ is thought to be determined by the excitation due to the energetic electrons, while those in higher excited states above $(n' \sim 5)$ may be governed by the EIR. In the medium excited state $(n' \sim 4)$, both the excitation and the EIR may have effects on that population. We can estimate the density of the energetic electrons in the heat pulse by analyzing the population densities (line emission intensities) with the collisional radiative model including the effect of the fast electrons, which will be discussed in the next section. $I_{sat}$ seems to rise more steeply comparing to that in Fig. 5, associated with the rapid weakness of the EIR.

The line intensity from the excited state $n' \sim 3$ peaks at $t \sim 1$ ms, and decreases in time, because the density and energy of the energetic electron component may be decreasing. From $t \sim 2.4$ ms, all line emission intensities from the excited states including $n' \sim 3$ are increasing. The population densities in all excited states are mainly governed by the EIR, associated with a decrease in $T_e$. However, although the EIR is enhanced at the latter half of the heat pulse, the effect of EIR is found to be *insufficient* to reduce ion particle flux to the target plate during the heat pulse at relatively low neutral pressure $P \sim 6.25$ mTorr. This increase in the ion particle flux should lead to increasing the heat load to the target plate because the ionization energy is released due to surface recombination on the target plate. Unfortunately, we do not have datum about the temporal evolution of the heat load to the target plate because the calorimetory method used to measure heat load in this experiment does not have sufficient time resolution to follow the short pulse.

When the heat pulse is off, $T_e$ drops from 0.3 eV to 0.2 eV, associated with the reduction of the discharge input power. A reduction of $T_e$ in high density plasma can provide a strong enhancement of the EIR, represented by a large increase in all emission intensities, and leading to a substantial reduction of ion particle flux to the target plate.

Figure 7 shows the time evolution for deeply detached plasma at relatively high neutral gas pressure $P \sim 9.26$ mTorr. At the beginning of the heat pulse, the time evolution

of $I_{sat}$, $T_e$, and the line emission intensities are similar to those in Fig. 6. However, at $t \sim 1.2$ ms, the ion particle flux to the target plate already starts to decrease and the line emission intensities from highly excited states are increasing. This indicates that the EIR can work well to suppress the increment of the ion flux induced by the heat pulse to the target plate because of the lower bulk electron temperature than that at $P \sim 6.25$ mTorr. It is found that the function of detached plasma regime due to the EIR during the heat pulse depends strongly on the electron cooling capability associated with the neutral pressure. When the heat pulse is off, the $I_{sat}$ drops by almost an order of magnitude, and the emission increases by a factor of 2, yet the drop in $T_e$ is barely perceptible. It seems unlikely that such a small change in $T_e$ could produce such a dramatic change in $I_{sat}$ because the recombination time is estimated to be on the order of 1 ms, as mentioned later. Another possible explanation will be presented in the next section.

## VI. DISCUSSION

In order to quantitatively specify the characteristics of energetic electrons in the heat pulse, we have analyzed the emission intensities from the excited states of a helium atom by using the CRAMD code,[17] including the effect of the energetic electrons (fast electrons). In the experimental conditions for detached plasmas corresponding to Figs. 6 and 7, the population densities of the excited states of a helium atom are thought to be governed by (i) EIR and (ii) electron impact excitation from the ground state due to the energetic electrons, because the contribution of bulk electrons for the excitation from the ground state is quite small in such a low electron temperature range less than 0.5 eV in the detached plasma conditions. Precise comparison between the change of the experimental spectra and the line intensities obtained with the CRAMD code may give us the quantitative information on the energetic electrons in the heat pulse.

Figure 8 shows the numerical results with the CRAMD code at $T_e \sim 0.3$ eV and $n_e \sim 10^{19}$ m$^{-3}$. Squares in Fig. 8(a) show the calculated emission intensities of the helium Balmer series from $n' \sim 3$ to 9, where the density of energetic electrons $n_b$ is assumed to be 0.1% of bulk electron density $n_e$ with the energy $E_b$ of 25 eV. Closed and open circles show the contributions of EIR and the electron impact excitation due to the energetic electrons, respectively. In this case, all emission intensities are found to come from the contribution of EIR, then the electron impact excitation due to the energetic electrons has little effect on the emission intensities. As $n_b$ increases to 0.5% of $n_e$, as shown in Fig. 8(b), the emission intensities from the excited states $n' \sim 3$ and 4 are found to be strongly influenced by the electron impact excitation due to the energetic electrons, while the EIR dominates in the emission intensities above $n' \sim 5$. With a further increase in $n_b$ to 1% of $n_e$, the emission intensities from the excited states $n' \sim 3$ to 5 are strongly enhanced with the electron impact excitation as shown in Fig. 8(c). On the other hand, the experimental results in Fig. 6 show that the emission intensities from $n' \sim 3$ and 4 are increasing at the beginning of the heat pulse, while the emission intensities of

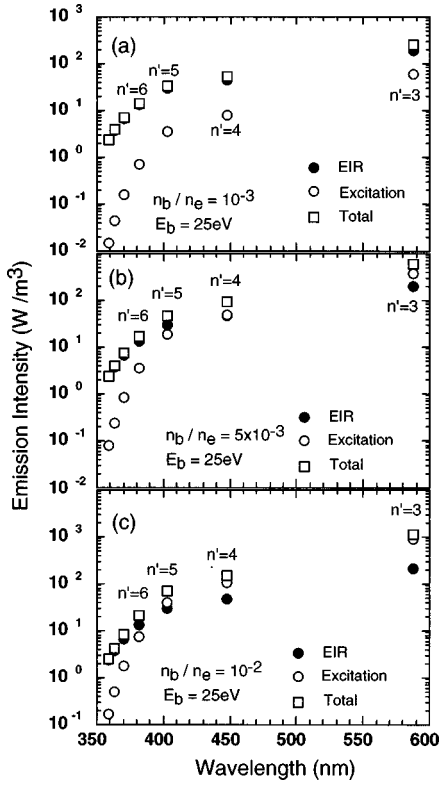


FIG. 8. Emission intensities of helium Balmer series obtained with the CRAMD code assuming $T_e \sim 0.3$ eV by taking account of electron beam component, whose density $n_b$ is (a) 0.1%, (b) 0.5%, and (c) 1% of the bulk plasma density $n_e \sim 10^{19}$ m$^{-3}$ with the energy $E_b$ of 25 eV. Closed and open circles are the calculated emission intensities due to EIR and the electron impact excitation with the energetic electrons, respectively.

the excited state above $n' \sim 5$ are not affected by the electron impact excitation in comparison with EIR. For example, if the energetic electrons with $n_b$ of 0.5% of the bulk plasma density and the energy $E_b$ of 25 eV corresponding to Fig. 8(b) are introduced to the detached plasma corresponding to Fig. 6, the emissions intensities from the excitation states $n' \sim 3$ and 4 can increase, because the electron impact excitation due to the energetic electrons can compensate the reduction of the emissions with EIR due to the increment of the bulk electron temperature from 0.3 eV to 0.4 eV at the beginning of the heat pulse; on the other hand, the emission intensities from the excited state above $n' \sim 5$ should decrease. Then, from the comparison between the experimental observations and the CRAMD's results, it may be concluded that the density of the energetic electrons at the beginning of the heat pulse is about 0.5% of the bulk electron density. Figure 9 shows the calculated emission intensities due to the electron impact excitation with the energetic electrons as a parameter of $E_b$, which shows a very weak dependence of relative Balmer series emission intensities on $E_b$ within the range 25–100 eV, which are thought to be reasonable value from the discharge voltage (93–105 V). These calculations also support the estimation of the density of the energetic electrons in the heat pulse mentioned above.

In probe measurements, if there is a significant population of hot electrons, which have Maxwellian distributions, two slopes clearly appear in semilogarithm plots of the

current–voltage characteristics. On the other hand, if there is significant electron beam component in the plasma, a kind of knee can be observed in the ion saturation current region. However, we cannot distinguish such indications in the current–voltage characteristics in our experiments. This is because the population of energetic electrons is small, as estimated above.

In Ref. 6, it has been pointed out that the energy transport parallel to the magnetic field is dominated by convection in the radiative divertor conditions. The heat flux due to the convection of energetic electrons with $n_b \sim 10^{17}$ m$^{-3}$ (0.5% of the bulk plasma density) and the energy $E_b$ of 25 eV is estimated to be $1.2\times10^6$ W/m$^2$ as $q_\parallel = n_b v_b E_b$, where $v_b$ is velocity of the energetic electrons. This value is larger than $q_\parallel$ due to the convection of bulk electrons in detached plasmas, thus the energy carried by the fast electrons exceeds that carried by the bulk electrons. This indicates that the behavior of the fast electrons during the heat pulse is key to understanding the dynamic response of the detached plasmas. At the cold electron temperatures observed in the detached plasmas, radiation is a negligible power loss, so it seems that the local plasma temperatures are being determined by the local rate of energy desorption from the fast electrons and the rate at which the neutrals can carry away the heat, because the energy of bulk electrons goes to the neutrals due to a strong electron–ion energy exchange process followed by ion–neutral elastic collisions and charge exchange processes.[22] For example, the mean free path of the fast neutral produced by the ion–neutral collisions until neutral–neutral collisions can be estimated to be $2.1\times10^{-2}$ m at $P\sim9.46$ mTorr, which is smaller than the distance between the plasma and the walls of the vacuum vessel. Then, neutral dynamics effects the transport of energy from plasmas to walls, which should be considered in a more precise analysis of the energy balance.

Next, we discuss the time scales and the evolution of line emission intensities during the plasma heat pulse. We will estimate characteristic times of the main processes that may be involved in our experimental results.

The plasma ion flow time scale is given by $\tau_i \sim L/u_i$, where $L$ is the length of the plasma in the divertor test region and $u_i$ is the ion flow velocity. Here, $\tau_i$ means the time for ions generated in the plasma source region to move to the target plate. In the Kundsen neutral transport regime, we have $u_i \sim C_S(\lambda_{in}/L)$, where $\lambda_{in}$ is the ion mean free path until ion–neutral collision, that is, $\lambda_{in} \sim 1/n_n\sigma_{in}$ ($n_n$ is the neutral density and $\sigma_{in}$ is the ion–neutral collision cross section), and $C_S \sim (T_e/M_i)^{0.5}$ ($M_i$ is the ion mass). For $L\sim2$ m, $T_e \sim 4$eV, $n_n \sim 10^{20}$ m$^{-3}$, and $\sigma_{\rm in} \sim 10^{-18}$ m$^{-2}$, we get $\tau_i \sim 3\times10^{-2}$ s. The characteristic time of ion flow is found to be much longer than the heat pulse duration time. This estimation indicates that we cannot explain the time evolution of the ion flux to the target plate by taking account of the ion convection alone.

Next, we consider the propagation of the plasma heat pulse through the electron channel, which is characterized by $\tau_e \sim L/u_e$, where $u_e$ is represented by $v_{Te}(\lambda_{ei}/L)$, which is an effective electron velocity describing heat pulse propagation ($v_{Te}$ and $\lambda_{ei}$ are the electron thermal velocity and the electron–ion mean free path, respectively). For $T_e\sim4$ eV and electron density $n_e \sim 3\times10^{18}$ m$^{-3}$, which correspond to the experimental datum at the discharge current of 24 A, we can estimate $\tau_e$ to be $10^{-4}$ s, which is much shorter compared to the heat pulse duration time and $\tau_i$. This electron time scale looks compatible with the time delay between the start-up times of $I_p$ and $I_{\rm sat}$. For the energetic electrons as described above, $\tau_e$ becomes much less than $10^{-4}$ s. In the detached plasma conditions, $\tau_e$ for bulk electrons must be much longer because $T_e$ is much lower and the mean free path between electrons and neutrals is shorter due to the higher neutral pressure. On the other hand, there is an undelayed start-up of $I_{\rm sat}$ to $I_p$ observed also in the detached case, as well as in the attached case, which seems to be inconsistent with $\tau_e$ for bulk electrons. From the above discussion, it may be concluded that the heat pulse generated in the plasma source region propagates through the energetic electrons with a time scale $\tau_e$ of less than $10^{-4}$ s, to heat up the bulk electrons and also to lead to an enhancement of the ionization (therefore, decrement of EIR) to increase plasma density all over the plasma column.

In general, the time scale $\tau_{saha}$ for relaxation of the population of highly excited states in the LTE condition is known to be less than $10^{-6}$ s,[25] almost instantaneous compared to the experimental time scale. So the distribution of excited states just follows the bulk electron temperature and density at each axial position, which guarantees the validity of the measurements of the time evolution of $T_e$ in detached recombining plasmas, as shown in Figs. 6 and 7.

The plasma recombination time scale $\tau_{\rm rec}$ is determined by $\tau_{\rm rec} \sim (v_{\rm rec})^{-1}$, where $v_{\rm rec} = \sigma_{\rm rec} n_e$ ($\sigma_{\rm rec}$ is the rate coefficient of EIR). Figure 10 shows $\tau_{\rm rec}$ as a function of $T_e$ with the electron density $n_e$ of $0.5\times10^{19}$ and $1.0\times10^{19}$ m$^{-3}$, respectively. For our experimental condition, $\tau_{\rm rec}$ may vary from $10^{-3}$ s to $3\times10^{-2}$ s depending on $T_e$. On the other hand, ionization time scale $\tau_{\rm ion}$ is quite large in a comparison with $\tau_{\rm rec}$, because the rate coefficient of the ionization process has a sharp drop with $T_e$. The above results mean that the volumetric plasma recombination has little effect on the time evolution of plasma density and $I_{\rm sat}$ during heat pulse at low neutral pressure $P\sim6.25$ mTorr because $\tau_{\rm rec}$ of 3

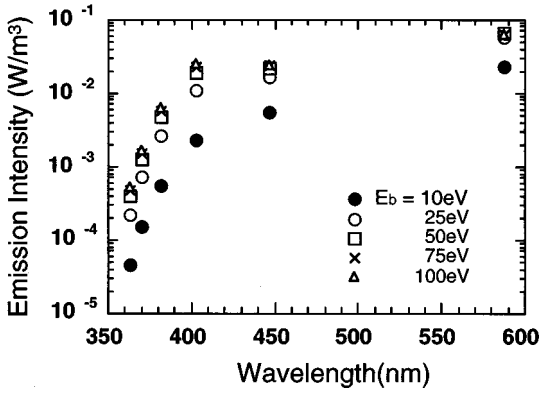


FIG. 9. Emission intensities of helium Balmer series with the electron impact excitation due to the electron beam component, whose density is $10^{19}$ m$^{-3}$ for different beam energy $E_b$.

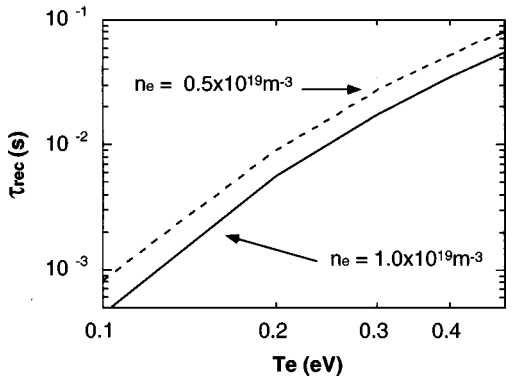


FIG. 10. Characteristic time for the plasma recombination as a function of electron temperature $T_e$.

$\times 10^{-2}$ s is longer than the duration time of the heat pulse. On the other hand, the plasma recombination has a strong influence at high neutral pressure $P \sim 9.46$ mTorr when $\tau_{\rm rec} \sim 10^{-3}$ s. When the heat pulse is off, the rapid cooling of the electron temperature associated with the high plasma density strongly enhances EIR even at low neutral pressure $P \sim 6.25$ mTorr, resulting in the strong reduction of $I_{\rm sat}$ because $\tau_{\rm rec}$ becomes less than $10^{-3}$ s. On the other hand, at $P \sim 9.46$ mTorr, the drop of $T_e$ is too small to explain the strong reduction of $I_{\rm sat}$. Another explanation should be sought. The fast electrons are able to provide ionization for highly excited neutrals, which are produced by recombination process. This means that the recombination process is getting weaker due to the reionization process by the fast electrons during the heat pulse. The sudden drop in the fast electrons suddenly reduces this ionization effect, and a net increase in recombination occurs even in the absence of a drop in the bulk $T_e$. If there are assumed to be fast electrons with an energy of 25 eV and a density of $1 \times 10^{17}$ m$^{-3}$ (0.5% of the bulk plasma density), the ionization time for excited helium atom ($n' \sim 6$) can be estimated to be $2.0 \times 10^{-6}$ s, where the ionization cross section from the highly excited level ($n' \sim 6$) is $1.7 \times 10^{-10}$ m$^2$, which can be roughly estimated using Lotz's empirical formula.[28] For helium atoms in more highly excited levels, the ionization time is getting smaller, which becomes comparable to the radiative decay time for these highly excited levels. This estimation suggests that reionization due to the fast electrons is playing a major role in the net recombination. In this case, neutral transport is also important because this reionization effect depends on how fast the highly excited atoms escape from the recombining region.

## V. CONCLUSION

We have performed experiments on a plasma heat pulse to the detached recombining helium plasma to demonstrate clearly the dynamic behavior of the volumetric plasma recombination in a linear divertor plasma simulator. The plasma heat pulse is generated by modulating the discharge current to produce energetic electrons in a plasma, which has strong effect on the line emissions from the low excited states of a helium atom. The density of the energetic electrons is estimated to be about 0.5% of the bulk electron density by comparing the population distribution over the principal quantum number obtained by the collisional radiative model (CRAMD code), including the effect of the energetic electrons with the experimental observations.

Overall physical pictures of dynamic response to the plasma heat pulse obtained by analyzing the time evolution of plasma parameters and Balmer-type spectra from helium atoms are as follows:

(a) At the beginning of the heat pulse, the electron temperature increases due to the rapid heat pulse propagation through the energetic electrons, leading to an increase in the plasma density because of the enhancement of the gas ionization.

(b) However, an increase in the plasma density results in faster cooling of the electrons and the electron temperature starts to drop.

(c) At a relatively low neutral pressure of 6.25 mTorr, the electron temperature does not drop below 0.2 eV during the heat pulse. The volumetric plasma recombination is not sufficient to suppress the increase in ion flux to the target plate because the time scale of the recombination is much longer than the duration time of the heat pulse. Therefore, the ion flux to the target plate is gradually increasing during the heat pulse due to the effects of both the ionization and the convection.

(d) At a high neutral pressure of 9.46 mTorr, the electron temperature is quite low before the heat pulse and the increment in $T_e$ at the start-up heat pulse is modest. Then, the volumetric plasma recombination works very effectively to start to reduce the ion flux to the target plate, even under the energetic electron injection to the system.

(e) After the heat pulse, the electron temperature rapidly drops because the additional input power to the electrons due to the heat pulse disappears. Moreover, both the insufficient heating and the faster electron cooling associated with the high plasma density makes $T_e$ below the initial value before the heat pulse, which strongly enhances the volumetric recombination at $P \sim 6.25$ mTorr, resulting in the strong reduction of the ion flux to the target plate in a high gas pressure. At $P \sim 9.46$ mTorr, the sudden drop in the fast electrons seems to reduce reionization for highly excited atoms produced by recombination, and a net increase in recombination occurs even in the absence of a drop in the bulk $T_e$, resulting in the reduction of the ion flux.

The function of the detached plasma regime with the radiative and three-body recombination during the heat pulse are strongly influenced by the electron cooling capability associated with the neutral pressure. Then, the kinetics of electrons including the energetic component in the detached plasma should be discussed from the point of the electron cooling. Furthermore, a neutral pressure sufficient to achieve plasma detachment in a steady state may not be sufficient to maintain detachment during a plasma heat pulse. Higher neutral pressure is required depending on the duration time of the plasma heat pulse.

## ACKNOWLEDGMENTS

The authors would like to express our deep gratitude to Dr. D. J. Sigmar, Dr. P. Catto, Dr. O. V. Batishchev, Dr. Y. Uesugi for their fruitful discussions and Mr. M. Takagi for his great technical support for this experiment. This work was supported by the Japan–U.S. collaboration program in the fusion area and also partly supported by the Ishida and Sumitomo foundations in Japan.

[1]D. Lumma, J. L. Terry, and B. Lipshultz, Phys. Plasmas **4**, 2555 (1997).
[2]R. Isler, G. R. McKee, N. H. Brooks, W. P. West, M. E. Fenstermacher, and R. W. Wood, Phys. Plasmas **4**, 2989 (1997).
[3]L. Schmits, B. Merriman, L. Blush, R. Lehmer, and R. W. Conn, Phys. Plasmas **2**, 3081 (1995).
[4]G. S. Chiu and S. A. Cohen, Phys. Rev. Lett. **76**, 1248 (1996).
[5]S. I. Krasheninnikov, A. Yu. Pigarov, D. A. Knoll, B. LaBombard, B. Lipshltz, D. J. Sigmar, T. K. Soboleva, J. L. Terry, and F. Wising, Phys. Plasmas **4**, 1638 (1997).
[6]W. Leonard, M. A. Mahdavi, S. L. Allen *et al.*, Phys. Rev. Lett. **78**, 4769 (1997).
[7]G. C. Vlases, J. M. Adams, P. Ageladarakis *et al.*, in *Proceedings of the 16th IAEA Fusion Energy Conference, Montreal, Canada, 1996* (The International Atomic Energy Agency, Vienna, 1997), Vol. 1, p. 371.
[8]K. Itami, N. Hosogane, N. Akasaka *et al.*, in *Proceedings of the 16th IAEA Fusion Energy Conference, Montreal, Canada, 1996* (The International Atomic Energy Agency, Vienna, 1997), Vol. 1, p. 385.
[9]V. Mertens, A. Herrmann, A. Kallenbach *et al.*, in *Proceedings of the 16th IAEA Fusion Energy Conference, Montreal, Canada, 1996* (The International Atomic Energy Agency, Vienna, 1997), Vol. 1, p. 413.
[10]M. A. Mahdavi, S. L. Allen, N. H. Brooks *et al.*, in *Proceedings of the 16th IAEA Fusion Energy Conference, Montreal, Canada, 1996* (The International Atomic Energy Agency, Vienna, 1997), Vol. 1, p. 397.
[11]N. Ezumi, N. Ohno, Y. Uesugi, J. Park, S. Watanabe, S. A. Cohen, S. I. Krasheninnikov, A. Yu. Pigarov, M. Takagi, and S. Takamura, in *Proceedings of the 24th European Physical Society Conference on Controlled Fusion and Plasma Physics, Berchtesgarden* (European Physical Society, Petit-Lancy, 1997), Vol. 21A, Part III, p. 1225.
[12]J. L. Terry, B. Lipschults, A. Yu. Pigarov, S. I. Krasheninnkov, B. LaBombard, D. Lumma, H. Ohkawa, D. Pappas, and M. Umansky, Phys. Plasmas **5**, 1759 (1997).
[13]J. Park, ''Studies on a transition to strongly recombining plasma,'' Ph.D. thesis, Princeton University, 1998.
[14]N. Ohno, N. Ezumi, S. Takamura, S. Krasheninnikov, and A. Pigarov, Phys. Rev. Lett. **81**, 818 (1998).
[15]S. I. Krasheninnikov, A. Yu. Pigarov, and D. J. Sigmar, Phys. Lett. A **214**, 285 (1996).
[16]D. E. Post, J. Nucl. Mater. **220-222**, 143 (1995).
[17]A. Yu. Pigarov and S. I. Krasheninnikov, Phys. Lett. A **222**, 251 (1996).
[18]O. Gruber, A. Kallenbach, M. Kaufman *et al.*, Phys Rev. Lett. **74**, 4217 (1995).
[19]G. L. Jackson, G. M. Staebler, S. L. Allen, *et al.*, J. Nucl. Mater. **241-243**, 618 (1997).
[20]G. Janeschitz, H. D Pacher, G. Federici *et al.*, in *Proceedings of the 16th IAEA Fusion Energy Conference, Montreal, Canada, 1996* (The International Atomic Energy Agency, Vienna, 1997), Vol. 2, p. 755.
[21]M. Otsuka, R. Ikee, and K. Ishii, J. Quant. Spectrosc. Radiat. Transf. **15**, 995 (1975).
[22]N. Ezumi, S. Mori, N. Ohno, M. Takagi, S. Takamura, and H. Suzuki, J. Nucl. Mater. **241-243**, 349 (1997).
[23]N. Ohno, S. Mori, N. Ezumi, M. Takagi, S. Takamura, and H. Suzuki, Contrib. Plasma Phys. **36**, 339 (1996).
[24]E. Hinnov and J. G. Hirshberg, Phys. Rev. **125**, 795 (1962).
[25]H. R. Griem, *Plasma Spectroscopy* (McGraw–Hill, New York, 1964).
[26]N. Ezumi, N. Ohno, K. Aoki, D. Nishijima, and S. Takamura, Contrib. Plasma Phys. **38**, S31 (1998).
[27]R. D. Monk, A. Loarte, A. Chankin, S. Clement, S. J. Davies, J. K. Ehrenberg, H. Y. Guo, J. Lingertat, G. F. Matthews, M. F. Stamp, and P. C. Stangeby, J. Nucl. Mater. **241-243**, 396 (1997).
[28]W. Lotz, Astrophys. J., Suppl. **14**, 207 (1967).